



HAL
open science

Simulation of rare-earth-doped high-power fiber-lasers using Matlab BVP solver

Stéphane Balac

► **To cite this version:**

Stéphane Balac. Simulation of rare-earth-doped high-power fiber-lasers using Matlab BVP solver. 2022. hal-03601902

HAL Id: hal-03601902

<https://hal.science/hal-03601902>

Preprint submitted on 8 Mar 2022

HAL is a multi-disciplinary open access archive for the deposit and dissemination of scientific research documents, whether they are published or not. The documents may come from teaching and research institutions in France or abroad, or from public or private research centers.

L'archive ouverte pluridisciplinaire **HAL**, est destinée au dépôt et à la diffusion de documents scientifiques de niveau recherche, publiés ou non, émanant des établissements d'enseignement et de recherche français ou étrangers, des laboratoires publics ou privés.

Simulation of rare-earth-doped high-power fiber-lasers using Matlab BVP solver

Stéphane Balac

UNIV. RENNES, CNRS, IRMAR-UMR 6625, F-35000 Rennes, France

Abstract

Numerical simulation of light-wave propagation in double-clad rare-earth-doped fiber-lasers implies dealing with a two-point boundary value problem (BVP) with non separated boundary conditions. We show that this BVP can be solved in a simple way using MATLAB BVP solver. However, this requires being able to provide to the BVP solver a relevant initial guess for the solution and the Jacobian matrix of the mapping defining the BVP. We show that when propagation losses and contribution to spontaneous emission are neglected, the BVP is equivalent to an initial value problem (IVP) whose solution, computed by MATLAB IVP solver, provides a suitable guess for MATLAB BVP solver. We also provide the expression of the Jacobian. This results in a very simple and cost-less MATLAB program for the simulation of light-wave propagation in high-power fiber-lasers.

Keywords: optics, optical fiber-lasers, rare-earth-doped fiber, boundary value problem, collocation method

2000 MSC: 78A60, 78M99, 65L10, 65L60

1. Introduction

In the theoretical study of high-power fiber-lasers, the most commonly used mathematical model is based on the rate-equation theory [2, 3] that describes the distributions of inversion populations and optical powers along the fiber when a stationary regime has been attained. In this model, the power propagation equations consist of several coupled non-linear first order ordinary differential equations (ODE) depending on the position z along the fiber [6]. The main difficulty for solving this system of non-linear ODE is related to the boundary conditions. We have a two-point boundary value problem (BVP), not an initial value problem (IVP), and the boundary conditions (BC) for this BVP are not separated, which means that we do not have independent relations at each endpoint for the unknowns but relations that correlate the values of the unknowns at the two endpoints, see relations (9c) and (9d) in the text below. This mathematical specificity is related to the reflection of the laser signal by Bragg mirrors at the two fiber extremities. Usually, existence and uniqueness for BVPs are much more difficult to investigate than for IVPs since there is no general theory [1]. As well, it is usually more difficult to solve numerically a BVP than an IVP where the solution can be propagated from one endpoint of the computational domain to the other. For a BVP, the solution is not fully known at the domain endpoints so that the numerical approach used for IVPs does not apply.

They are mainly two approaches for solving a BVP. The first one is to use a shooting method [10, 1]. Basically, shooting methods consist in reducing the solving of the BVP to the solving of a sequence of IVPs where the values for the missing boundary conditions at the fiber front end ($z = 0$) are enforced. After the missing boundary values were chosen arbitrarily at the

first attempt (the initial guess), they are adjusted for the next attempts by comparing the computed back end ($z = L$) boundary values to the BVP boundary conditions and using a root finding solver to compute the new boundary values at $z = 0$ for the next iteration. The second approach is to use collocation methods [1, 10]. The collocation technique introduces a mesh of points to divide the fiber length into sub-intervals. Over each sub-interval, an approximation formula for the system of ODE is considered. It can be a Runge-Kutta formula or a Lobatto formula as used in MATLAB BVP solvers [7]. This results in a global system of non-linear algebraic equations to which the relations given by the boundary conditions are added. Then, this system of non-linear equations is solved to obtain the approximate solution to the BVP.

In the last years, several authors have proposed numerical strategies to solve the BVP stemming from the modeling of light-wave propagation in high-power fiber-lasers. Among the more recent papers, one can quote reference [8] where the standard shooting approach described above is improved by using some relations (close to relations (A.2) given in Appendix A) between the boundary values of the pump and laser signal powers at the both ends of the fiber. The main drawback of the method identified by the authors is that it is necessary for the initial guessed power laser to be lower than the true (unknown) value for the method to converge fast and provide accurate results. In [12], the authors also use a shooting method but they combined it with a relaxation method to improve the convergence speed of the shooting method. We can also quote references [4, 5] where a complicated strategy is deployed to solve the BVP using MATLAB BVP solver. For an incomprehensible reason, the authors use MATLAB BVP solver in conjunction with an iterative method where, starting from guessed initial values and updating these values at each step, convergence to the so-

Email address: stephane.balac@univ-rennes1.fr (Stéphane Balac)

lution to the BVP is expected. Although, according to their authors, these different numerical approaches provide the expected results in terms of simulation of light-wave propagation in high-power fiber-lasers, they appear to be excessively and unnecessarily complicated from a numerical point of view, especially the numerical approaches suggested in references [12, 4, 5]. Moreover, all these numerical approaches are very dependent on the initial guess for the iterative strategies they use and it is well known that fixed-point like methods efficiency is very dependent on the quality of the initial guess, see e.g. [13, chap.14] or [1, chap. 8].

In this paper, we show that it is possible to use MATLAB BVP solver, in a very simple way, to solve the BVP stemming from the modeling of light-wave propagation in double-clad rare-earth-doped fiber-lasers. Moreover, we show that an initial guess for MATLAB BVP solver, close to the solution to the BVP, can be obtained at a very low cost. Indeed, when propagation losses and spontaneous emission are neglected, we show that an equivalent IVP to the BVP at hand can be obtained, for which the solution can be computed simply by using MATLAB ode45 solver. This leads to a very simple and efficient MATLAB program to simulate light-wave propagation in rare-earth-doped high-power fiber-lasers.

The document is organized as follows. In Section 2, we introduce the mathematical model for light-wave propagation in rare-earth-doped high-power fiber-lasers giving rise to the BVP with non-separated BC. Then, in Section 3, we explain how to use MATLAB BVP solver in an efficient way to solve this BVP. Namely, we discuss the way an initial guess required by MATLAB BVP solver can be computed so as to be close to the solution for a faster convergence of MATLAB BVP solver and we give the expression of the Jacobian also required by MATLAB BVP solver for a better efficiency. Section 4 is dedicated to an overview of the SHPOL program written for the simulation of light-wave propagation in rare-earth-doped high-power fiber-lasers. Finally, in Section 5, we compare the results provided by SHPOL program to the existing literature results for validation purposes.

2. The mathematical model

We denote by L the length of the fiber and we assume that the axis of the fiber coincides with the z -axis of the reference frame. Using the rate-equation theory under the steady state condition [2, 3], we obtain a set of coupled equations for the pump and signal laser co-propagative and contra-propagative powers $P_p^+, P_p^-, P_s^+, P_s^-$ describing light-wave propagation in a linear cavity as follows [6]:

$$\begin{cases} \pm \frac{dP_p^\pm}{dz}(z) = ((\sigma_p^{(e)} + \sigma_p^{(a)}) N_2(z) - \sigma_p^{(a)} N) \Gamma_p P_p^\pm(z) \\ \quad - \alpha_p P_p^\pm(z) \end{cases} \quad (1a)$$

$$\begin{cases} \pm \frac{dP_s^\pm}{dz}(z) = ((\sigma_s^{(e)} + \sigma_s^{(a)}) N_2(z) - \sigma_s^{(a)} N) \Gamma_s P_s^\pm(z) \\ \quad - \alpha_s P_s^\pm(z) + \Gamma_s \sigma_e^{(s)} P_0 N_2(z) \end{cases} \quad (1b)$$

where

- P_p^\pm and P_s^\pm represent respectively the pump power (index p) at pump wavelength λ_p and the signal laser power (index s) at laser wavelength λ_s in the forward propagating direction (superscript $+$) and backward propagating direction (superscript $-$);
- Γ_p and Γ_s are respectively the overlap integral factors between the ion-doping distribution and mode fields of pump and signal laser lights;
- $\sigma_p^{(a)}$ and $\sigma_p^{(e)}$ denote respectively the absorption and emission cross-sections at the pump wavelength λ_p ;
- $\sigma_s^{(a)}$ and $\sigma_s^{(e)}$ denote respectively the absorption and emission cross-sections at the signal laser wavelength λ_s ;
- α_p and α_s represent the propagation losses coefficients including background loss and scattering loss at the pump and signal laser wavelengths respectively;
- P_0 represents the contribution to spontaneous emission into the propagation laser mode;
- N is the doping substance concentration density assumed to be constant along the fiber and N_2 is the upper-level population density.

For continuous-wave laser, the upper-level population density N_2 at position z (in unit m^{-3}) is given by [2, 6]:

$$N_2(z) = \frac{\sigma_s^{(a)} \frac{\Gamma_s}{h\nu_s} P_s(z) + \sigma_p^{(a)} \frac{\Gamma_p}{h\nu_p} P_p(z)}{\frac{A_{\text{eff}}}{\tau} + (\sigma_s^{(a)} + \sigma_s^{(e)}) \frac{\Gamma_s}{h\nu_s} P_s(z) + (\sigma_p^{(a)} + \sigma_p^{(e)}) \frac{\Gamma_p}{h\nu_p} P_p(z)} N \quad (2)$$

where $P_p(z) = P_p^+(z) + P_p^-(z)$ is the total pump power and $P_s(z) = P_s^+(z) + P_s^-(z)$ is the total signal power, τ is the spontaneous emission lifetime, A_{eff} is the effective doping area, $h = 6.62607015 \cdot 10^{-34} \text{ J} \cdot \text{s}$ is the Planck constant and $\nu_p = c/\lambda_p$, $\nu_s = c/\lambda_s$, where $c = 299\,792\,458 \text{ m} \cdot \text{s}^{-1}$ denotes light velocity in vacuum, are respectively the pump and signal frequencies. The contribution to spontaneous emission is given by $P_0 = 2hc^2 \delta_\lambda / \lambda_s^3$ where δ_λ is the spontaneous emission bandwidth.

We define the pump attenuation constant $\alpha_p^{(a)}$ and the signal attenuation constant $\alpha_s^{(a)}$ (in unit m^{-1}) as

$$\alpha_p^{(a)} = N \Gamma_p \sigma_p^{(a)} \quad (3a)$$

$$\alpha_s^{(a)} = N \Gamma_s \sigma_s^{(a)} \quad (3b)$$

and the saturation powers for the pump and signal (in unit W) as

$$P_p^{\text{sat}} = \frac{A_{\text{eff}} h \nu_p}{\tau (\sigma_p^{(a)} + \sigma_p^{(e)}) \Gamma_p} \quad (4a)$$

$$P_s^{\text{sat}} = \frac{A_{\text{eff}} h \nu_s}{\tau (\sigma_s^{(a)} + \sigma_s^{(e)}) \Gamma_s} \quad (4b)$$

Using the above defined quantities, the ion population density N_2 given by (2) can be expressed as

$$N_2(z) = \frac{\tau}{A_{\text{eff}}} \frac{\frac{\alpha_p^{(a)}}{h\nu_p} P_p(z) + \frac{\alpha_s^{(a)}}{h\nu_s} P_s(z)}{1 + \frac{P_s(z)}{P_s^{\text{sat}}} + \frac{P_p(z)}{P_p^{\text{sat}}}} \quad (5)$$

Substituting N_2 as given by (5) into the propagation equations (1), we obtain the following non-linear system of ODE

$$\begin{cases} \pm \frac{dP_p^\pm}{dz}(z) = -(\alpha_p^{(a)} + \alpha_p) P_p^\pm(z) + G_p(P_p^\pm(z), P_s^\pm(z)) \frac{P_p^\pm(z)}{P_p^{\text{sat}}} \\ \pm \frac{dP_s^\pm}{dz}(z) = -(\alpha_s^{(a)} + \alpha_s) P_s^\pm(z) \\ \quad + G_s(P_p^\pm(z), P_s^\pm(z)) \left(\frac{P_s^\pm(z)}{P_s^{\text{sat}}} + \frac{P_0}{P_s^{\text{sat},e}} \right) \end{cases} \quad (6a)$$

where (we recall that $P_p = P_p^+ + P_p^-$ and $P_s = P_s^+ + P_s^-$)

$$G_p(P_p^\pm(z), P_s^\pm(z)) = \frac{\alpha_p^{(a)} P_p(z) + \frac{\nu_p}{\nu_s} \alpha_s^{(a)} P_s(z)}{1 + \frac{P_s(z)}{P_s^{\text{sat}}} + \frac{P_p(z)}{P_p^{\text{sat}}}} \quad (7a)$$

$$G_s(P_p^\pm(z), P_s^\pm(z)) = \frac{\alpha_s^{(a)} P_s(z) + \frac{\nu_s}{\nu_p} \alpha_p^{(a)} P_p(z)}{1 + \frac{P_s(z)}{P_s^{\text{sat}}} + \frac{P_p(z)}{P_p^{\text{sat}}}} \quad (7b)$$

and where, with reference to (4b), we have set

$$P_s^{\text{sat},e} = \frac{A_{\text{eff}} h \nu_s}{\tau \sigma_s^{(e)} \Gamma_s} \quad (8)$$

The boundary conditions (BC) are as follows [6]:

$$\begin{cases} P_p^+(0) = R_p^{(1)} P_p^-(0) + P_{\text{pump}}^+ \\ P_p^-(L) = R_p^{(2)} P_p^+(L) + P_{\text{pump}}^- \end{cases} \quad (9a)$$

$$\begin{cases} P_p^-(L) = R_p^{(2)} P_p^+(L) + P_{\text{pump}}^- \end{cases} \quad (9b)$$

$$\begin{cases} P_s^+(0) = R_s^{(1)} P_s^-(0) \end{cases} \quad (9c)$$

$$\begin{cases} P_s^-(L) = R_s^{(2)} P_s^+(L) \end{cases} \quad (9d)$$

where P_{pump}^+ and P_{pump}^- are the pump powers available at the front ($z = 0$) and back ($z = L$) ends respectively, $R_s^{(1)}$ and $R_s^{(2)}$ are respectively the front and back ends mirror reflectivities at the signal wavelength λ_s and $R_p^{(1)}$ and $R_p^{(2)}$ are the reflectivities at the pump wavelength λ_p .

Thus, we have to solve a BVP that consists in the non-linear first order coupled ODE (6) and linear two-point BC (9). The specificity of these BC is that they are not separated due to the reflection at the fiber ends that mixes forward and backward propagating powers. However, this BVP can be solved in a very simple way under MATLAB using its BVP solvers contrary to what has been stated in [8, 12, 4, 5] and without need of complicated numerical approaches. To this end, we express BVP (6)–(9) in the form

$$Y'(z) = F(Y(z)) \quad \forall z \in]0, L[\quad (10)$$

where the unknown vector $Y(z) \in \mathbb{R}^4$ is defined as

$$Y(z) = \begin{pmatrix} P_p^+(z) & P_p^-(z) & P_s^+(z) & P_s^-(z) \end{pmatrix}^\top \in \mathbb{R}^4$$

where \top indicates matrix transposition and the mapping F is defined as

$$F : Y \in \mathbb{R}^4 \mapsto \begin{pmatrix} -(\alpha_p^{(a)} + \alpha_p) Y_1 + G_p(Y) \frac{Y_1}{P_p^{\text{sat}}} \\ (\alpha_p^{(a)} + \alpha_p) Y_2 - G_p(Y) \frac{Y_2}{P_p^{\text{sat}}} \\ -(\alpha_s^{(a)} + \alpha_s) Y_3 + G_s(Y) \left(\frac{Y_3}{P_s^{\text{sat}}} + \frac{P_0}{P_s^{\text{sat},e}} \right) \\ (\alpha_s^{(a)} + \alpha_s) Y_4 - G_s(Y) \left(\frac{Y_4}{P_s^{\text{sat}}} + \frac{P_0}{P_s^{\text{sat},e}} \right) \end{pmatrix} \quad (11)$$

where here and throughout the paper Y_1, \dots, Y_4 denotes the components of Y . The BC (9) can be expressed in matrix form as

$$M_0 Y(0) + M_L Y(L) = \begin{pmatrix} P_{\text{pump}}^+ \\ P_{\text{pump}}^- \\ 0 \\ 0 \end{pmatrix} \quad (12)$$

where the two matrices M_0 and M_L in $\mathcal{M}_4(\mathbb{R})$ are given by

$$M_0 = \begin{pmatrix} 1 & -R_p^{(1)} & 0 & 0 \\ 0 & 0 & 0 & 0 \\ 0 & 0 & 1 & -R_s^{(1)} \\ 0 & 0 & 0 & 0 \end{pmatrix} \quad M_L = \begin{pmatrix} 0 & 0 & 0 & 0 \\ -R_p^{(2)} & 1 & 0 & 0 \\ 0 & 0 & 0 & 0 \\ 0 & 0 & -R_s^{(2)} & 1 \end{pmatrix}$$

3. MATLAB BVP solvers

MATLAB BVP solver `bvp4c` implements a collocation method based on the three-stage Lobatto IIIa formula, see [7]. MATLAB BVP solver `bvp5c` implements the four-stage Lobatto IIIa formula and slightly differs from `bvp4c` on some internal implementation choices, see MATLAB documentation for details. MATLAB BVP solvers efficiency is improved when an initial guess close enough to the solution is provided and when the Jacobian matrix of the function F defining the ODE given by (11) is available. We examine now these two topics for BVP (6)–(9).

Propagation losses in the fiber, although not negligible, are generally small and they contribute lowly to the BVP solution that is mainly driven by other optical phenomena. The same can be observed concerning the contribution to spontaneous emission into the propagation laser mode. This observation leads us to chose as initial guess for MATLAB BVP solver, the solution to BVP (6)–(9) in the case when $\alpha_p = \alpha_s = 0$ and $P_0 = 0$. This idea would be idiotic if solving the BVP under these assumptions was as difficult as solving the complete BVP, but such is not the case. Indeed, we show in Appendix A that when losses and spontaneous emission are neglected, BVP (6)–(9) can be reformulated in an equivalent Initial Value Problem (IVP) that can be solved easily using standard numerical method such as the Runge-Kutta RK4 method as e.g. implemented in MATLAB `ode45` solver [11]. This solution, though different from the real solution to the BVP is likely to be close to it and it will thus provide a very good initial guess for MATLAB BVP solvers. Therefore, using MATLAB `ode45` solver, we solve the IVP composed of ODE (6) and initial conditions (A.9) for $P_p^-(0)$, (A.10) for $P_s^-(0)$, (9a) for $P_p^+(0)$ and (9c) for $P_p^-(0)$. Then, we provide to MATLAB BVP solver `bvp4c`, as initial guess, the solution Y to this IVP computed at the grid nodes of a subdivision $(z_j)_{j=0, \dots, J}$ of the interval $[0, L]$.

Let us now consider the calculation of the Jacobian matrix J_F of the mapping F introduced in (11). For all $Y \in \mathbb{R}^4$, we have

$$J_F(Y) = \begin{pmatrix} \partial_1 F_1(Y) & \partial_2 F_1(Y) & \partial_3 F_1(Y) & \partial_4 F_1(Y) \\ \partial_1 F_2(Y) & \partial_2 F_2(Y) & \partial_3 F_2(Y) & \partial_4 F_2(Y) \\ \partial_1 F_3(Y) & \partial_2 F_3(Y) & \partial_3 F_3(Y) & \partial_4 F_3(Y) \\ \partial_1 F_4(Y) & \partial_2 F_4(Y) & \partial_3 F_4(Y) & \partial_4 F_4(Y) \end{pmatrix} \quad (13)$$

where ∂_j refers to the partial derivation with respect to the j -th variable and F_i refers to the i -th component of the mapping F . A straightforward calculation shows that the partial derivatives of F are given for $j \in \{1, \dots, 4\}$ and for $Y \in \mathbb{R}^4$ by

$$\begin{aligned}\partial_j F_1(Y) &= -(\alpha_p^{(a)} + \alpha_p) \delta_{1,j} + \frac{G_p(Y)}{P_p^{\text{sat}}} \delta_{1,j} + \frac{Y_1}{P_p^{\text{sat}}} \partial_j G_p(Y) \\ \partial_j F_2(Y) &= (\alpha_p^{(a)} + \alpha_p) \delta_{2,j} - \frac{G_p(Y)}{P_p^{\text{sat}}} \delta_{2,j} - \frac{Y_2}{P_p^{\text{sat}}} \partial_j G_p(Y) \\ \partial_j F_3(Y) &= -(\alpha_s^{(a)} + \alpha_s) \delta_{3,j} + \frac{G_s(Y)}{P_s^{\text{sat}}} \delta_{3,j} + \left(\frac{Y_3}{P_s^{\text{sat}}} + \frac{P_0}{P_s^{\text{sat},e}} \right) \partial_j G_s(Y) \\ \partial_j F_4(Y) &= (\alpha_s^{(a)} + \alpha_s) \delta_{4,j} - \frac{G_s(Y)}{P_s^{\text{sat}}} \delta_{4,j} - \left(\frac{Y_4}{P_s^{\text{sat}}} + \frac{P_0}{P_s^{\text{sat},e}} \right) \partial_j G_s(Y)\end{aligned}$$

where $\delta_{i,j}$ denotes the Kronecker symbol (equal to 1 when $i = j$ and 0 otherwise). The partial derivatives of the mappings G_p and G_s defined in (7) are given by

$$\begin{aligned}\partial_1 G_p(Y) &= \partial_2 G_p(Y) = \left(\alpha_p^{(a)} - \frac{G_p(Y)}{P_p^{\text{sat}}} \right) \frac{1}{\psi(Y)} \\ \partial_3 G_p(Y) &= \partial_4 G_p(Y) = \left(\frac{\nu_p}{\nu_s} \alpha_s^{(a)} - \frac{G_p(Y)}{P_s^{\text{sat}}} \right) \frac{1}{\psi(Y)}\end{aligned}$$

and

$$\begin{aligned}\partial_1 G_s(Y) &= \partial_2 G_s(Y) = \left(\frac{\nu_s}{\nu_p} \alpha_p^{(a)} - \frac{G_s(Y)}{P_p^{\text{sat}}} \right) \frac{1}{\psi(Y)} \\ \partial_3 G_s(Y) &= \partial_4 G_s(Y) = \left(\alpha_s^{(a)} - \frac{G_s(Y)}{P_s^{\text{sat}}} \right) \frac{1}{\psi(Y)}\end{aligned}$$

where $\psi(Y) = 1 + \frac{Y_1 + Y_2}{P_p^{\text{sat}}} + \frac{Y_3 + Y_4}{P_s^{\text{sat}}}$.

4. The SHIPOL program

A MATLAB program based on the ideas presented above has been implemented. It can be downloaded with its documentation from HAL library at the following URL : <https://hal.archives-ouvertes.fr/hal-03212156>

The program basically consists in the following stages :

1. Computation of a guess (rough approximate solution) by solving ODE (6) with $\alpha_s = \alpha_p = P_0 = 0$ under the initial conditions given by (A.9) for $P_p^-(0)$, (A.10) for $P_s^-(0)$, (9a) for $P_p^+(0)$ and (9c) for $P_s^+(0)$ using MATLAB ode45 solver.
2. Solving of the BVP (10) with BC (12) by MATLAB bvp4c solver with the guess computed at stage 1. Efficiency of bvp4c is improved by supplying the Jacobian matrix of the mapping F to bvp4c.
3. Results display. Values of the pump and signal powers in the forward and backward directions (P_p^+ , P_p^- , P_s^+ , P_s^-) at the two fiber ends are shown as well as the value of the total laser signal output power. Graphical display of the pump and signal powers in the forward and backward directions as a function of the position z along the fiber together with the ratio N_2/N are also provided.

The accuracy of the computed solution can be evaluated using an error estimator based on relations (A.1). We must have $P_p^+(0) P_p^-(0) = P_p^+(L) P_p^-(L)$ and, when $P_0 = 0$, we must also have $P_s^+(0) P_s^-(0) = P_s^+(L) P_s^-(L)$. Therefore, we use as error estimator

$$\mathfrak{E}_P = \left| \frac{P_p^+(0) P_p^-(0) - P_p^+(L) P_p^-(L)}{P_p^+(0) P_p^-(0) + P_p^+(L) P_p^-(L)} \right| \quad (14a)$$

$$\mathfrak{E}_S = \left| \frac{P_s^+(0) P_s^-(0) - P_s^+(L) P_s^-(L)}{P_s^+(0) P_s^-(0) + P_s^+(L) P_s^-(L)} \right| \quad (14b)$$

where \mathfrak{E}_S is relevant only when $P_0 \equiv 0$. The closer to zero these estimators are, the more accurate the computation can be expected to be.

5. Numerical validation

We have compared the simulation results provided by the SHIPOL program to several results available in the literature. (The numerical methods used in these papers are not always detailed and the codes are not available for further comparisons.) The numerical results presented below were obtained using the software MATLAB (R2018b) under Linux-Ubuntu OS on an Intel Core i5 computer with 8 Go RAM.

5.1. Simulation of light-wave propagation in a Yb³⁺ doped fiber-laser

Parameter	Notation	Value
Fiber length	L	50 m
Pump wavelength	λ_p	$9.2 \cdot 10^{-7}$ m
Signal wavelength	λ_s	$1.09 \cdot 10^{-6}$ m
Pump power at front end	P_{pump}^+	20 W
Pump power at the back end	P_{pump}^-	0 W
Pump overlap factor	Γ_p	$1.2 \cdot 10^{-3}$
Signal overlap factor	Γ_s	$8.2 \cdot 10^{-1}$
Doping substance concentration	N_f	$4 \cdot 10^{25}$ ions/m ³
Pump absorption cross section	$\sigma_p^{(a)}$	$6 \cdot 10^{-25}$ m ²
Pump emission cross section	$\sigma_p^{(e)}$	$2.5 \cdot 10^{-26}$ m ²
Signal absorption cross section	$\sigma_s^{(a)}$	$1.4 \cdot 10^{-27}$ m ²
Signal emission cross section	$\sigma_s^{(e)}$	$2 \cdot 10^{-25}$ m ²
Pump background losses	α_p	$3 \cdot 10^{-3}$ m ⁻¹
Signal background losses	α_s	$5 \cdot 10^{-3}$ m ⁻¹
Front mirror reflectivity at λ_p	$R_p^{(1)}$	0
Output mirror reflectivity at λ_p	$R_p^{(2)}$	0
Front mirror reflectivity at λ_s	$R_s^{(1)}$	0.98
Output mirror reflectivity at λ_s	$R_s^{(2)}$	0.04
Lifetime of the upper-level atoms	τ	10^{-3} s
Effective mode area	A_{eff}	$5 \cdot 10^{-11}$ m ²

Table 1: Parameter values for the Yb³⁺ doped fiber-laser investigated in [6].

We have considered the Yb³⁺-doped fiber-laser investigated in [6], the parameters of which are given in Table 1. The ASE is neglected in [6] so that we set $P_0 \equiv 0$ in (1b). We have depicted in Fig. 1 the pump and signal powers in the forward and

backward directions, *i.e.* $P_p^+, P_p^-, P_s^+, P_s^-$, as a function of the position along the fiber together with the ratio $N_2(z)/N$. This figure is identical to [6, Fig. 8]. We have obtained a forward signal power at $z = 0$ with value $P_s^+(0) = 2.02871$ W and a backward signal power at $z = 0$ with value $P_s^-(0) = 2.07011$ W. At the fiber back end $z = L$, the values are $P_s^+(L) = 10.2465$ W and $P_s^-(L) = 0.409861$ W. The forward pump power at $z = L$ is 4.15728 W whereas the backward pump power remains zero along the fiber. The CPU time for the simulation was 1.8 s and the error estimator defined in (14b) was $\mathfrak{E}_s = 2.7418 \cdot 10^{-12}$. (Note that the estimator \mathfrak{E}_p not relevant here since $P_p^- \equiv 0$.) Taking into account the ASE in the simulation, we have obtained $P_s^+(0) = 2.02874$ W, $P_s^-(0) = 2.07014$ W, $P_s^+(L) = 10.2466$ W and $P_s^-(L) = 0.409862$ W. These values are not significantly different from the one obtained by neglecting the ASE which justify the assumption made in [6]. We want to point out that the numerical method used in [6] to solve the BVP is not specified as it is mentioned only for comparison purposes with a semi-analytical approach valid under strong pumping conditions, such that the signal power is high enough to saturate the gain medium and suppress the spontaneous emission.

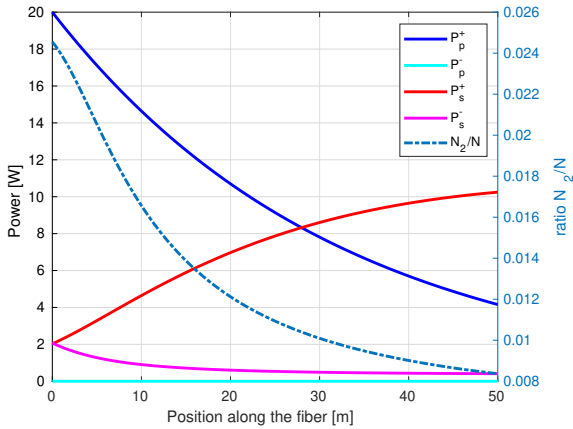


Figure 1: Pump and signal powers in the forward and backward directions $P_p^+, P_p^-, P_s^+, P_s^-$ as a function of the position along the fiber for the Yb^{3+} fiber-laser the parameters of which are given in Table 1 (left axis). Ratio $N_2(z)/N$ as a function of the position along the fiber in dotted line and right axis.

As a complement, we have made a simulation for the Yb^{3+} doped fiber-laser investigated in [8]. The parameters of the fiber are similar to the one given in Table 1 excepted that the fiber length is $L = 150$ m, the pump power launched into the front end P_{pump}^+ is 1000 W and the signal background losses are $\alpha_s = 3 \cdot 10^{-3} \text{ m}^{-1}$. We have depicted in Fig. 2 the pump and signal powers in the forward and backward directions $P_p^+, P_p^-, P_s^+, P_s^-$ as a function of the position along the fiber together with the ratio $N_2(z)/N$. We have obtained a forward signal power at $z = 0$ with value $P_s^+(0) = 105.493$ W and a backward signal power at $z = 0$ with value $P_s^-(0) = 107.645$ W. At the fiber back end $z = L$, the values are $P_s^+(L) = 532.818$ W and $P_s^-(L) = 21.3127$ W. The forward pump power at $z = L$ is 8.84451 W whereas the backward pump power remains zero along the fiber. The CPU time for the simulation was 0.7 s and

the error estimator defined in (14b) was $\mathfrak{E}_s = 1.6709 \cdot 10^{-11}$.

Fig. 2 is to be compared with [8, Fig. 2]. The two figures are significantly different. Since the only difference with the previous simulation that matches the results published in [6] is the fiber length and pump power launched at the fiber front end, we infer that Fig. 2 in [8] do not correspond to the fiber parameter values provided in the text in [8] or that the numerical method presented in [8] is implemented in an erroneous way or that the method itself is erroneous. It should be noted that we have detected an other error in [8] in the results reported for the thulium-doped fiber-laser, see Section 5.3.

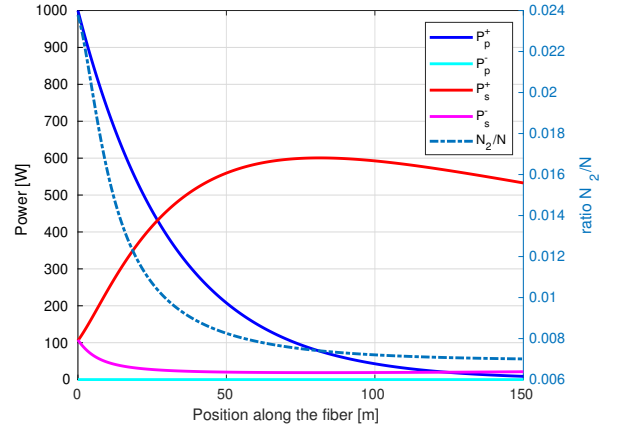


Figure 2: Pump and signal powers in the forward and backward directions $P_p^+, P_p^-, P_s^+, P_s^-$ as a function of the position along the fiber for the Yb^{3+} doped fiber-laser considered in [8].

5.2. Simulation of light-wave propagation in a Nd^{3+} doped fiber-laser

We then have compared the results obtained by our numerical method to the one given in [6] for a Nd^{3+} -doped high-power double-clad fiber laser characterized by the values given in Table 2. We have depicted in Fig. 3 the pump and signal powers in the forward and backward directions, *i.e.* $P_p^+, P_p^-, P_s^+, P_s^-$, as a function of the position along the fiber together with the ratio $N_2(z)/N$. This figure is identical to the one depicted in [6, Fig. 5]. We have obtained a forward signal power at $z = 0$ with value $P_s^+(0) = 2.50126$ W and a backward signal power at $z = 0$ with value $P_s^-(0) = 2.5523$ W. At the fiber back end $z = L$, the values are $P_s^+(L) = 12.6333$ W and $P_s^-(L) = 0.505331$ W. The forward pump power at $z = L$ is 2.19664 W whereas the backward pump power remains zero along the fiber. The CPU time for the simulation was 0.6 s and the error estimator defined in (14b) was $\mathfrak{E}_s = 2.6426 \cdot 10^{-12}$. (Note that the estimator \mathfrak{E}_p is not relevant here since $P_p^- \equiv 0$.)

For comprehensiveness, we have also made a simulation when the pump is injected at the fiber back end $z = L$, *i.e.* $P_p^+(0) = 0$ and $P_p^-(L) = 20$ W, the other parameters are as given in Table 2. The result is depicted in Fig. 4 and it is identical to the one depicted in [6, Fig. 6].

Parameter	Notation	Value
Fiber length	L	50 m
Pump wavelength	λ_p	$0.808 \cdot 10^{-6}$ m
Signal wavelength	λ_s	$1.060 \cdot 10^{-6}$ m
Pump power at front end	P_{pump}^+	20 W
Pump power at back end	P_{pump}^-	0 W
Pump overlap factor	Γ_p	0.01
Signal overlap factor	Γ_s	0.8
Doping substance concentration	N_f	$2 \cdot 10^{24}$ ions/m ³
Pump absorption cross section	$\sigma_p^{(a)}$	$2 \cdot 10^{-24}$ m ²
Pump emission cross section	$\sigma_p^{(e)}$	0 m ²
Signal absorption cross section	$\sigma_s^{(a)}$	0 m ²
Signal emission cross section	$\sigma_s^{(e)}$	$2.5 \cdot 10^{-24}$ m ²
Pump background losses	α_p	$4.5 \cdot 10^{-3}$ m ⁻¹
Signal background losses	α_s	0 m ⁻¹
Front mirror reflectivity at λ_p	$R_p^{(1)}$	0
Output mirror reflectivity at λ_p	$R_p^{(2)}$	0
Front mirror reflectivity at λ_s	$R_s^{(1)}$	0.98
Output mirror reflectivity at λ_s	$R_s^{(2)}$	0.04
Lifetime of the upper-level atoms	τ	$4 \cdot 10^{-4}$ s
Effective mode area	A_{eff}	$1 \cdot 10^{-11}$ m

Table 2: Parameter values for the Nd³⁺ doped fiber-laser investigated in [6].

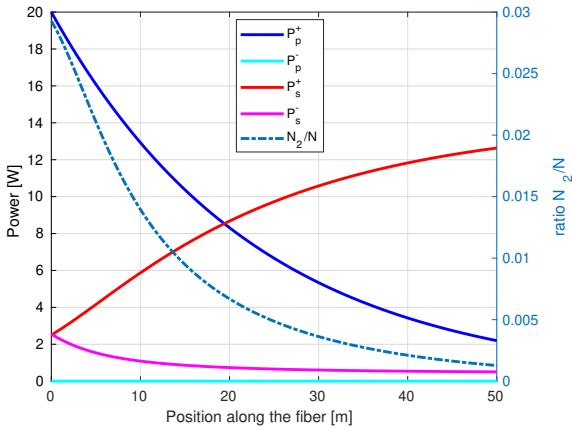


Figure 3: Pump and signal powers in the forward and backward directions P_p^+ , P_p^- , P_s^+ , P_s^- as a function of the position along the fiber for the Nd³⁺ fiber-laser the parameters of which are given in Table 2 (left axis). Ratio $N_2(z)/N$ as a function of the position along the fiber in dotted line and right axis.

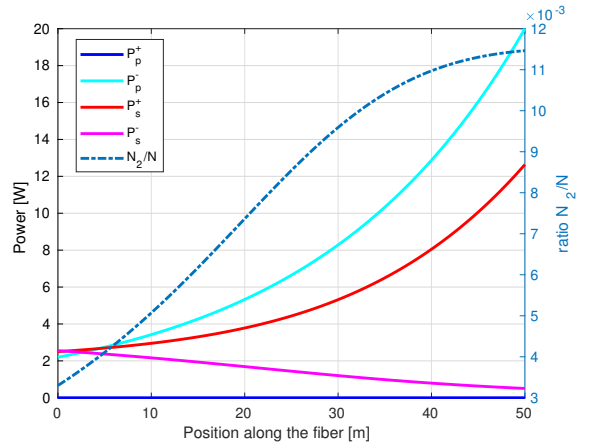


Figure 4: Pump and signal powers in the forward and backward directions P_p^+ , P_p^- , P_s^+ , P_s^- as a function of the position along the fiber for the Nd³⁺ fiber-laser the parameters of which are given in Table 2 except that the pump is injected at $z = L$ (left axis). Ratio $N_2(z)/N$ as a function of the position along the fiber in dotted line and right axis.

5.3. Simulation of light-wave propagation in a thulium-doped fiber-laser

Finally, we have considered the Tm^{3+} -doped high-power double-clad fiber-laser proposed in [8] characterized by the values given in Table 3. The ASE is neglected in [8] so that we set $P_0 \equiv 0$ in the simulation. Note that the doping substance concentration given in [8] was $N = 4.68 \cdot 10^{26}$ ions/m³ and it is changed for $N = 8.6 \cdot 10^{25}$ ions/m³ to comply with the value of the literature quoted in [8].

Parameter	Notation	Value
Fiber length	L	25 m
Pump wavelength	λ_p	$0.790 \cdot 10^{-6}$ m
Signal wavelength	λ_s	$1.973 \cdot 10^{-6}$ m
Pump power at front end	P_{pump}^+	1000 W
Pump power at back end	P_{pump}^-	0 W
Pump overlap factor	Γ_p	0.01
Signal overlap factor	Γ_s	0.752
Doping substance concentration	N_t	$8.6 \cdot 10^{25}$ ions/m ³
Pump absorption cross section	$\sigma_p^{(a)}$	$5 \cdot 10^{-25}$ m ²
Pump emission cross section	$\sigma_p^{(e)}$	0 m ²
Signal absorption cross section	$\sigma_s^{(a)}$	$1 \cdot 10^{-26}$ m ²
Signal emission cross section	$\sigma_s^{(e)}$	$2.5 \cdot 10^{-25}$ m ²
Pump background losses	α_p	$3 \cdot 10^{-3}$ m ⁻¹
Signal background losses	α_s	$5 \cdot 10^{-3}$ m ⁻¹
Front mirror reflectivity at λ_p	$R_p^{(1)}$	0
Output mirror reflectivity at λ_p	$R_p^{(2)}$	0
Front mirror reflectivity at λ_s	$R_s^{(1)}$	0.98
Output mirror reflectivity at λ_s	$R_s^{(2)}$	0.04
Lifetime of the upper-level atoms	τ	$1.45 \cdot 10^{-5}$ s
Effective mode area	A_{eff}	$1.39 \cdot 10^{-11}$ m

Table 3: Parameter values for the Tm^{3+} doped fiber-laser investigated in [8].

We have depicted in Fig. 5 the pump and signal powers in the forward and backward directions (P_p^+ , P_p^- , P_s^+ , P_s^-) as a function of the position along the fiber together with the ratio $N_2(z)/N$. This figure is quite similar to the one depicted in [8, Fig. 5]. Note however that when using the doping substance concentration given in [8] ($N = 4.68 \cdot 10^{26}$ ions/m³) rather than the one given in Table 3, the figure we obtain is significantly different from [8, Fig. 5]. We have obtained a forward signal power at $z = 0$ with value $P_s^+(0) = 74.8308$ W and a backward signal power at $z = 0$ with value $P_s^-(0) = 76.358$ W. At the fiber back end $z = L$, the values are $P_s^+(L) = 377.953$ W and $P_s^-(L) = 15.1181$ W. The forward pump power at $z = L$ is 2.02216 W whereas the backward pump power remains zero along the fiber. The CPU time for the simulation was 1.3 s and the error estimator defined in (14b) was $\mathfrak{E}_s = 7.5682 \cdot 10^{-12}$. Note that when the ASE was taken into account in the simulation, we obtained similar results to the one provided above which justify the assumption made in [8] to neglect the ASE.

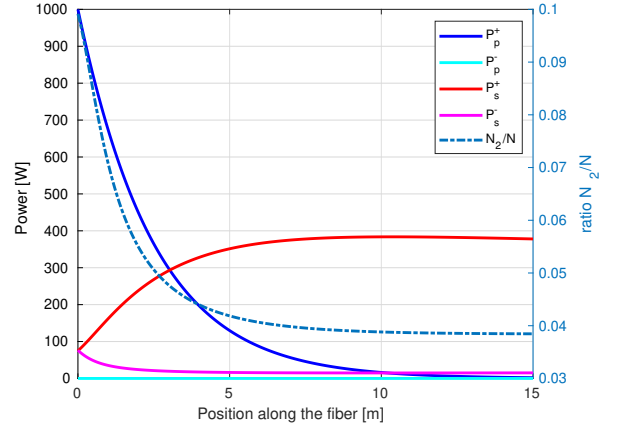


Figure 5: Pump and signal powers in the forward and backward directions P_p^+ , P_p^- , P_s^+ , P_s^- as a function of the position along the fiber for the Tm^{3+} doped fiber-laser.

6. Conclusion

We have shown that the boundary value problem (BVP) stemming from the modeling of light-wave propagation in high-power fiber-lasers can be solved in a simple way by MATLAB BVP solver. This approach renders meaningless the numerical methods proposed in [8, 12, 4, 5] to solve this BVP. The effectiveness of the method relies on the efficiency of MATLAB BVP solver program and on the practicability to provide an initial guess close to the solution to the BVP at a very low cost as shown in the paper. Moreover we have provided the expression of the Jacobian of the mapping defining the BVP that further improves the overall effectiveness of the simulation. This results in a very simple and efficient MATLAB program for the simulation of light-wave propagation in high-power fiber-lasers. We hope that the author MATLAB program distributed under CeCILL-C free software license, will benefit to the greatest number of researchers in the optics community.

Acknowledgments

The author would like to thanks Prof. Thierry Chartier, from Foton Laboratory, ENSSAT-University of Rennes 1 (France), for having drawn attention to this numerical problem and for fruitful discussions on fiber-lasers.

Appendix A. An equivalent initial value problem in the absence of losses

We consider in this appendix the special case when the losses and the contribution to spontaneous emission into the propagation laser mode can be neglected. That is to say, we consider BVP (6)–(9) under the assumptions that $\alpha_s = \alpha_p = 0$ and $P_0 = 0$.

In this special case, the solutions P_p^\pm, P_s^\pm to the set of ODE (6) exhibit the following features: There exist two real numbers C_p

and C_s such that for all $z \in [0, L]$

$$P_p^+(z) P_p^-(z) = C_p, \quad P_s^+(z) P_s^-(z) = C_s. \quad (\text{A.1})$$

This property can be easily proved by considering the mapping $z \in [0, L] \mapsto P_p^+(z) P_p^-(z)$ and showing that its derivative is zero. We have

$$\frac{d}{dz} (P_p^+(z) P_p^-(z)) = P_p^+(z) \frac{dP_p^-}{dz}(z) + P_p^-(z) \frac{dP_p^+}{dz}(z).$$

We then sum equation (6a) for P_p^+ preparatorily multiplied by P_p^- and equation (6a) for P_p^- preparatorily multiplied by P_p^+ to show that the derivative is zero. Note that the properties (A.1) are true even when the losses are not zero. However, when $P_0 \neq 0$, only the relation on P_p^\pm remains valid.

We deduce from (A.1) and from BC (9a) and (9b), the following relationships between the boundary values at the fiber ends:

$$P_p^+(L) = \frac{1}{R_p^{(2)}} \left(\frac{1}{4} (P_{\text{pump}}^-)^2 + R_p^{(1)} R_p^{(2)} (P_p^-(0))^2 + P_{\text{pump}}^- R_p^{(2)} P_p^-(0) \right)^{\frac{1}{2}} - \frac{P_{\text{pump}}^-}{2R_p^{(2)}} \quad (\text{A.2a})$$

$$P_s^+(L) = \sqrt{\frac{R_s^{(1)}}{R_s^{(2)}}} P_s^-(0) \quad (\text{A.2b})$$

Note that when $R_p^{(2)} = 0$, (A.2a) has to be changed for

$$P_{\text{pump}}^- P_p^+(L) = R_p^{(1)} (P_p^-(0))^2 + P_{\text{pump}}^- P_p^-(0). \quad (\text{A.3})$$

Let us now show how we can express the two quantities $P_p^-(0)$ and $P_s^-(0)$ in terms of the fiber-laser characteristic parameters. By difference between (1a) considered for P_p^+ and P_p^- on the one hand and by difference between (1b) considered for P_s^+ and P_s^- on the other hand, one can easily show that N_2 given by (2) can be expressed as

$$N_2(z) = -\frac{\tau_3}{h A_{\text{eff}}} \left(\frac{1}{v_p} \left(\frac{dP_p^+}{dz}(z) - \frac{dP_p^-}{dz}(z) \right) + \frac{1}{v_s} \left(\frac{dP_s^+}{dz}(z) - \frac{dP_s^-}{dz}(z) \right) \right). \quad (\text{A.4})$$

Substituting this expression of N_2 into equations (1a)–(1b), we obtain

$$\left\{ \begin{aligned} \pm \frac{dP_p^\pm}{dz}(z) &= - \left(\frac{dP_p^\pm}{dz}(z) - \frac{dP_p^\mp}{dz}(z) \right) \frac{P_p^\pm(z)}{P_p^{\text{sat}}} \\ &\quad - \frac{v_p}{v_s} \left(\frac{dP_s^\pm}{dz}(z) - \frac{dP_s^\mp}{dz}(z) \right) \frac{P_p^\pm(z)}{P_p^{\text{sat}}} - \alpha_p^a P_p^\pm(z) \end{aligned} \right. \quad (\text{A.5a})$$

$$\left\{ \begin{aligned} \pm \frac{dP_s^\pm}{dz}(z) &= - \frac{v_s}{v_p} \left(\frac{dP_p^\pm}{dz}(z) - \frac{dP_p^\mp}{dz}(z) \right) \frac{P_s^\pm(z)}{P_s^{\text{sat}}} \\ &\quad - \left(\frac{dP_s^\pm}{dz}(z) - \frac{dP_s^\mp}{dz}(z) \right) \frac{P_s^\pm(z)}{P_s^{\text{sat}}} - \alpha_s^a P_s^\pm(z) \end{aligned} \right. \quad (\text{A.5b})$$

Let us consider equation (A.5a) for P_p^+ . We divide both sides by $P_p^+(z)$ under the assumption that the forward pump power P_p^+ never cancels and we integrate over the interval $[0, L]$:

$$\int_0^L \frac{1}{P_p^+(z)} \frac{dP_p^+(z)}{dz} dz = -\frac{1}{P_p^{\text{sat}}} \int_0^L \left(\frac{dP_p^+}{dz}(z) - \frac{dP_p^-}{dz}(z) \right) dz - \frac{v_p}{v_s P_p^{\text{sat}}} \int_0^L \left(\frac{dP_s^+}{dz}(z) - \frac{dP_s^-}{dz}(z) \right) dz - \alpha_p^a L.$$

It follows that

$$\log \left(\frac{P_p^+(L)}{P_{\text{pump}}^+ + R_p^{(1)} P_p^-(0)} \right) = -\frac{1}{P_p^{\text{sat}}} \left(P_p^+(L) - P_{\text{pump}}^+ - R_p^{(1)} P_p^-(0) - P_{\text{pump}}^- - R_p^{(2)} P_p^+(L) + P_p^-(0) \right) - \frac{v_p}{v_s P_p^{\text{sat}}} \left(P_s^+(L) - R_s^{(1)} P_s^-(0) - R_s^{(2)} P_s^+(L) + P_s^-(0) \right) - \alpha_p^a L.$$

The same calculation can be done with the three other equations in (A.5a)–(A.5b). Taking into account relations (A.2), it remains the following two equations for the unknowns $P_p^-(0)$ and $P_s^-(0)$:

$$\left\{ \begin{aligned} \log \left(\frac{P_{\text{pump}}^+ + R_p^{(1)} P_p^-(0)}{\phi(P_p^-(0))} \right) &= \frac{v_p}{v_s} \frac{\eta}{P_p^{\text{sat}}} P_s^-(0) + \alpha_p^a L \\ &\quad + \frac{1}{P_p^{\text{sat}}} \Phi(P_p^-(0)) \end{aligned} \right. \quad (\text{A.6a})$$

$$\frac{1}{2} \log(R_s^{(1)} R_s^{(2)}) = \frac{\eta}{P_s^{\text{sat}}} P_s^-(0) + \alpha_s^a L + \frac{v_s}{v_p} \frac{1}{P_s^{\text{sat}}} \Phi(P_p^-(0)) \quad (\text{A.6b})$$

where we have set

$$\eta = \sqrt{\frac{R_s^{(1)}}{R_s^{(2)}}} - R_s^{(1)} - \sqrt{R_s^{(1)} R_s^{(2)}} + 1$$

$$\Phi(P_p^-(0)) = (1 - R_p^{(2)}) \phi(P_p^-(0)) + (1 - R_p^{(1)}) P_p^-(0) - (P_{\text{pump}}^+ + P_{\text{pump}}^-)$$

$$\phi(P_p^-(0)) = \sqrt{\left(\frac{P_{\text{pump}}^-}{2R_p^{(2)}} \right)^2 + \frac{R_p^{(1)}}{R_p^{(2)}} (P_p^-(0))^2 + \frac{P_{\text{pump}}^- P_p^-(0)}{R_p^{(2)}}} - \frac{P_{\text{pump}}^-}{2R_p^{(2)}}$$

Combining equations (A.6a) and (A.6b), we obtain that

$$\log \left(\frac{P_{\text{pump}}^+ + R_p^{(1)} P_p^-(0)}{\phi(P_p^-(0))} \right) = A \quad (\text{A.7})$$

where

$$A = \frac{v_p P_s^{\text{sat}}}{v_s P_p^{\text{sat}}} \left(\frac{1}{2} \log(R_s^{(1)} R_s^{(2)}) - \alpha_s^a L \right) + \alpha_p^a L \quad (\text{A.8})$$

From (A.7), we deduce that $P_p^-(0)$ is solution to the following algebraic equation with unknown X

$$\sqrt{\frac{1}{4} (P_{\text{pump}}^-)^2 + R_p^{(1)} R_p^{(2)} X^2 + P_{\text{pump}}^- R_p^{(2)} X} - e^{-A} R_p^{(1)} R_p^{(2)} = e^{-A} R_p^{(2)} P_{\text{pump}}^+ + \frac{1}{2} P_{\text{pump}}^-.$$

Solving this algebraic equation, we obtain that its non-negative solution reads

$$P_p^-(0) = \frac{P_{\text{pump}}^+ R_p^{(2)} + P_{\text{pump}}^- e^A}{e^{2A} - R_p^{(1)} R_p^{(2)}} \quad (\text{A.9})$$

Then, from (A.6b), we have

$$P_s^-(0) = \frac{P_s^{\text{sat}}}{\eta} \left(\frac{1}{2} \log(R_s^{(1)} R_s^{(2)}) - \frac{\nu_s}{\nu_p} \frac{1}{P_s^{\text{sat}}} \Phi(P_p^-(0)) - \alpha_s^a L \right). \quad (\text{A.10})$$

Finally, under the assumption that $\alpha_s = \alpha_p = 0$ and $P_0 = 0$, the BVP (6)–(9) is equivalent to the IVP composed of the ODE (6) and initial conditions (A.9) for $P_p^-(0)$, (A.10) for $P_s^-(0)$, (9a) for $P_p^+(0)$ and (9c) for $P_p^-(0)$.

Note that in [6] the authors also propose an IVP, different of the one proposed here, equivalent to the BVP (6)–(9) under the following additional assumptions: $\sigma_s^{(a)} \ll \sigma_p^{(a)}$, $\sigma_p^{(e)} = 0$ and $R_p^{(1)} = R_p^{(2)} = 0$. We did not need these additional assumptions here. As well, in [9] the authors proposed an analytical solution to the BVP in the absence of losses but also require additional assumptions.

References

- [1] U. ASCHER, R. MATTHEI, AND R. RUSSELL, *Numerical Solution of Boundary Value Problems for Ordinary Differential Equations*, Classics in Applied Mathematics, Society for Industrial and Applied Mathematics, 1994.
- [2] P. BECKER, A. OLSSON, AND J. SIMPSON, *Erbium-Doped Fiber Amplifiers: Fundamentals and Technology*, Optics and Photonics, Elsevier Science, 1999.
- [3] E. DESURVIRE, *Erbium-Doped Fiber Amplifiers: Principles and Applications*, Wiley Series in Telecommunications and Signal Processing, Wiley, 2002.
- [4] X. HU, T. NING, L. PEI, Q. CHEN, AND W. JIAN, *Number sequence transition method based on Matlab BVP solvers for high power Yb3+ doped fiber lasers*, Optics & Laser Technology, 58 (2014), pp. 76–83.
- [5] X. HU, T. NING, L. PEI, Q. CHEN, AND J. LI, *A simple error control strategy using Matlab BVP solvers for Yb3+ doped fiber lasers*, Optik, 126 (2015), pp. 3446–3451.
- [6] I. KELSON AND A. A. HARDY, *Strongly pumped fiber lasers*, IEEE Journal of Quantum Electronics, 34 (1998), pp. 1570–1577.
- [7] J. KIERZENKA AND L. F. SHAMPINE, *A BVP solver based on residual control and the Matlab PSE*, ACM Trans. Math. Softw., 27 (2001), pp. 299–316.
- [8] J. LIU, C. ZHAO, S. WEN, D. FAN, AND C. SHUAI, *An improved shooting algorithm and its application to high-power fiber lasers*, Optics Communications, 283 (2010), pp. 3764–3767.
- [9] M. PEYSOKHAN, E. MOBINI, AND A. MAFI, *Analytical formulation of a high-power Yb-doped double-cladding fiber laser*, OSA Continuum, 3 (2020), pp. 1940–1951.
- [10] L. SHAMPINE, I. GLADWELL, AND S. THOMPSON, *Solving ODEs with MATLAB*, Cambridge University Press, 2003.
- [11] L. F. SHAMPINE AND M. W. REICHEL, *The Matlab ODE suite*, SIAM Journal on Scientific Computing, 18 (1997), pp. 1–22.
- [12] L. SHANG, L. QI, Y. LIAO, AND S. ZHANG, *A combined algorithm for simulating fiber lasers based on the shooting and relaxation methods*, Optical Fiber Technology, 18 (2012), pp. 502–508.
- [13] C. UEBERHUBER, *Numerical Computation 2: Methods, Software, and Analysis*, Springer, 1997.